RESEARCH ARTICLE

PMP22 exon 4 deletion causes ER retention of PMP22 and a gain-of-function allele in CMT1E

David S. Wang[1,a], Xingyao Wu[1,a], Yunhong Bai[1], Craig Zaidman[2], Tiffany Grider[1,3], John Kamholz[3], James R. Lupski[4], Anne M. Connolly[2] & Michael E. Shy[1,3]

[1]Department of Neurology, Neuromuscular Division, University of Iowa Hospitals and Clinics, Iowa City, Iowa
[2]Departments of Neurology and Pediatrics, Neuromuscular Division, Washington University School of Medicine, St. Louis, Missouri
[3]Department of Neurology, Neurogenetics Division, University of Iowa Hospitals and Clinics, Iowa City, Iowa
[4]Department of Pediatrics, Baylor College of Medicine, Houston, Texas

Correspondence
Michael E. Shy, Department of Neurology, Carver College of Medicine, 200 Hawkins Drive Iowa City, Iowa 52242.
Tel: 319-353-5097; Fax: 319-356-7009;
E-mail: michael-shy@uiowa.edu

[a]The two authors contributed equally to the manuscript.

Abstract

Objective: To determine whether predicted fork stalling and template switching (FoSTeS) during mitosis deletes exon 4 in peripheral myelin protein 22 KD (PMP22) and causes gain-of-function mutation associated with peripheral neuropathy in a family with Charcot–Marie–Tooth disease type 1E. **Methods**: Two siblings previously reported to have genomic rearrangements predicted to involve exon 4 of *PMP22* were evaluated clinically and by electrophysiology. Skin biopsies from the proband were studied by RT-PCR to determine the effects of the exon 4 rearrangements on exon 4 mRNA expression in myelinating Schwann cells. Transient transfection studies with wild-type and mutant PMP22 were performed in Cos7 and RT4 cells to determine the fate of the resultant mutant protein. **Results**: Both affected siblings had a sensorimotor dysmyelinating neuropathy with severely slow nerve conduction velocities (<10 m/sec). RT-PCR studies of Schwann cell RNA from one of the siblings demonstrated a complete in-frame deletion of *PMP22* exon 4 (PMP22Δ4). Transfection studies demonstrated that PMP22Δ4 protein is retained within the endoplasmic reticulum and not transported to the plasma membrane. **Conclusions**: Our results confirm that that FoSTeS-mediated genomic rearrangement produced a deletion of exon 4 of PMP22, resulting in expression of both PMP22 mRNA and protein lacking this sequence. In addition, we provide experimental evidence for endoplasmic reticulum retention of the mutant protein suggesting a gain-of-function mutational mechanism consistent with the observed CMT1E in this family. PMP22Δ4 is another example of a mutated myelin protein that is misfolded and contributes to the pathogenesis of the neuropathy.

Introduction

Charcot–Marie–Tooth (CMT) disease is the most common inherited peripheral neuropathy affecting approximately 1:2500 individuals.[1] Roughly half of these patients have CMT1A,[2] a demyelinating neuropathy caused by a 1.4-Mb duplication in chromosome 17p12 that contains the peripheral myelin protein 22 gene, *PMP22*, an integral membrane protein expressed in PNS compact myelin.[3,4] CMT1A is hypothesized to occur as a result of nonallelic homologous recombination (NAHR)[5–7] in a region of 17p12 surrounding and including the *PMP22* gene, causing increased expression of the normal gene product.

Point mutations in *PMP22* gene can cause a relatively severe demyelinating or dysmyelinating peripheral neuropathy, in which myelin never forms normally during development. Mutations within the *PMP22* gene are classified as CMT1E.[2] Most CMT1E mutations are missense mutations probably resulting in a gain-of-new protein function.[8] In contrast, some *PMP22* point mutations

produce a loss-of-protein function by a shift in the protein reading frame, leading to premature termination of translation.[9–12] A similar loss of function can also be caused by the reciprocal deletion of PMP22 within 17p12 that caused the CMT1A duplication. Loss of PMP22 function leads to an electrophysiologically distinct inherited neuropathy known as hereditary neuropathy with pressure palsies.[13]

Recently, it was proposed that abnormalities of fork stalling and template switching (FoSTeS) or microhomology-mediated break-induced replication (MMBIR) caused a complex rearrangement within an individual *PMP22* allele that resulted in CMT1 in a family in which two siblings, but neither parent, developed CMT1.[14] The rearrangements were identified in DNA from white blood cells and were hypothesized to result from three separate FoSTeS/MMBIR-mediated template switching events that were predicted to specifically disrupt the sequence of *PMP22* exon 4 in the patients. The mother was found to be mosaic for the same rearrangement with lower levels in the mutated allele in her WBC. Both siblings had markedly reduced nerve conduction velocities, whereas the conduction velocities of the mother were normal.

We had the opportunity to examine both affected siblings and further test this hypothesis by evaluating *PMP22* expression from myelinated nerves obtained from skin biopsies. RT-PCR analysis from the skin biopsies revealed the absence of exon 4 sequences in PMP22 mRNA, consistent with the analysis of genomic DNA as described by Zhang and coworkers. Transfection studies demonstrated that the mutant protein is retained in the endoplasmic reticulum, which is the most parsimonious explanation for its pathogenesis via a gain-of-function mutational mechanism.

Methods

Clinical evaluation

The two siblings were evaluated clinically at the University of Iowa CMT clinic at ages 9 and 13 years. Neurological examination and neurophysiological and skin biopsy studies were performed on the patients during their clinic visit. A skin biopsy was obtained following informed consent as part of an orthopedic procedure at Washington University, St. Louis. Informed consent according to the Declaration of Helsinki and the Institutional Review Boards at the participating centers approving the study was obtained from both siblings and their parents.

Skin biopsy and RT-PCR

The skin sample was evaluated as described previously.[15] The sample was treated in freshly prepared RNALater (Qiagen, CA, Cat. No.: 1017980). RNA was isolated with RNeasy Micro Kit (Qiagen, CA, Cat. No.: 74004) followed by the RT reaction in SuperScript First-Strand Synthesis System for RT-PCR (Invitrogen, CA, Cat. No.: 12371-019) and then the PCR in Platinum Pfx DNA Polymerase (Invitrogen, CA, Cat. No.: 11708-013). The upstream and downstream primers were 5′-GGGCAGAAACTCCGCT-GAGCAGAA-3′ and 5′-GTACGCTCAGCGCCTCAGACA-GAC-3′, respectively. PCR conditions were 95°C 2 min/ 95°C 15°sec, 60°C 30°sec, 68°C 1 min for 35 cycles/68°C 10 min. Sanger sequencing was performed to analyze the products after cloning with Zero Blunt TOPO PCR Cloning Kit with One Shot TOP10 Electrocamp Chemically Competent *Escherichia coli* (Invitrogen, CA, Cat. No.: K2860-20).

Preparation of wild-type and mutant PMP22 constructions

The cDNAs encoding both wild-type and mutant human PMP22 mRNA sequences were synthesized from the patient's skin biopsy RNA by RT-PCR and cloned into an expression vector with an HA tag at its 3′ end (Cat. No.: A921149-1, Lucigen Corp. Middleton, WI). The HA tag was obtained from the pME-HA vector (Cat. No.: A921149-1). Both of these constructs were used in the transfection studies described below.

Cell culture, transfection, and immunocytochemistry

Cos 7 cells (American Type Culture Collection) and RT4 rat Schwann cells (Gift from Dr. John Svaren) were separately grown on four-well chamber slides in Dulbecco's modified Eagle's medium supplemented with 10% fetal bovine serum and 1% penicillin–streptomycin and transfected with 2-µg plasmid DNA using Lipofectamine™ 3000 (Invitrogen). Cells were transfected with the following plasmids: (1) WT-PMP22, (2) PMP22-exon 4 deletion – each plasmid with the hemagglutinin epitope tag fused to the N-terminus. Forty-eight hours after transfection, immunocytochemistry was carried out as described previously[16]). In brief, cells were rinsed twice in PBS for 5 min and then fixed in 4% paraformaldehyde for 5 min. After being washed three times in PBS, cells were incubated with primary antibodies at 4°C overnight: Antihemagglutinin (anti-HA), 1:1000 (Cell Signaling Technology® Cat#2367 [mouse]; #3724 [rabbit]); anticalnexin (marker for endoplasmic reticulum), 1:300 (Abcam, Cat# ab22595); antigiantin (marker for Golgi apparatus), 1:300 (Abcam, Cat# ab37266). Following three 10-min washes in PBS and 1 h incubation with secondary antibodies (Cy3-conjugated donkey anti-rabbit IgG, Jackson Immuno Research, Cat#711-165-152 or anti-mouse,

Cat#711-165-1521; fluorescein [FITC]-conjugated Affini-Pure Donkey anti-mouse IgG, cat#712-095-151; or anti-rabbit IgG cat#711-095-152), the coverslips were mounted applying Anti-Fade 4-6-diamino-2-phenylindole (DAPI) mounting media that labeled nuclei (Invitrogen Cat# P36931).

We determined the transfection efficiency by taking 10 images under 40 × objective lens per group; WT-PMP22 and PMP22-exon 4 deletion. HA-tag-labeled cells were counted as a positively transfected cell. We then divided this number by total nuclei number stained with DAPI. Transfected RT4 cells were imaged (× 63 magnification, repeated 3 times) magnification with a Zeiss 710 confocal microscope in order to demonstrate cell surface expression, endoplasmic reticulum or Golgi retention of

PMP22-exon 4 deletion mutation or PMP22wt. The number of colocalized cells that showed overlap of HA-PMP22 and ER or Golgi was divided by the total number of transfected cells to obtain percentage of colocalization.

Results

Clinical summary

We evaluated two sisters who had been previously demonstrated to have complex rearrangement of PMP22 exon 4 that they had inherited from their asymptomatic mother who was mosaic for this unusual mutation.[17] Both sisters had evidence of a significant sensorimotor dysmyelinating peripheral neuropathy that began in
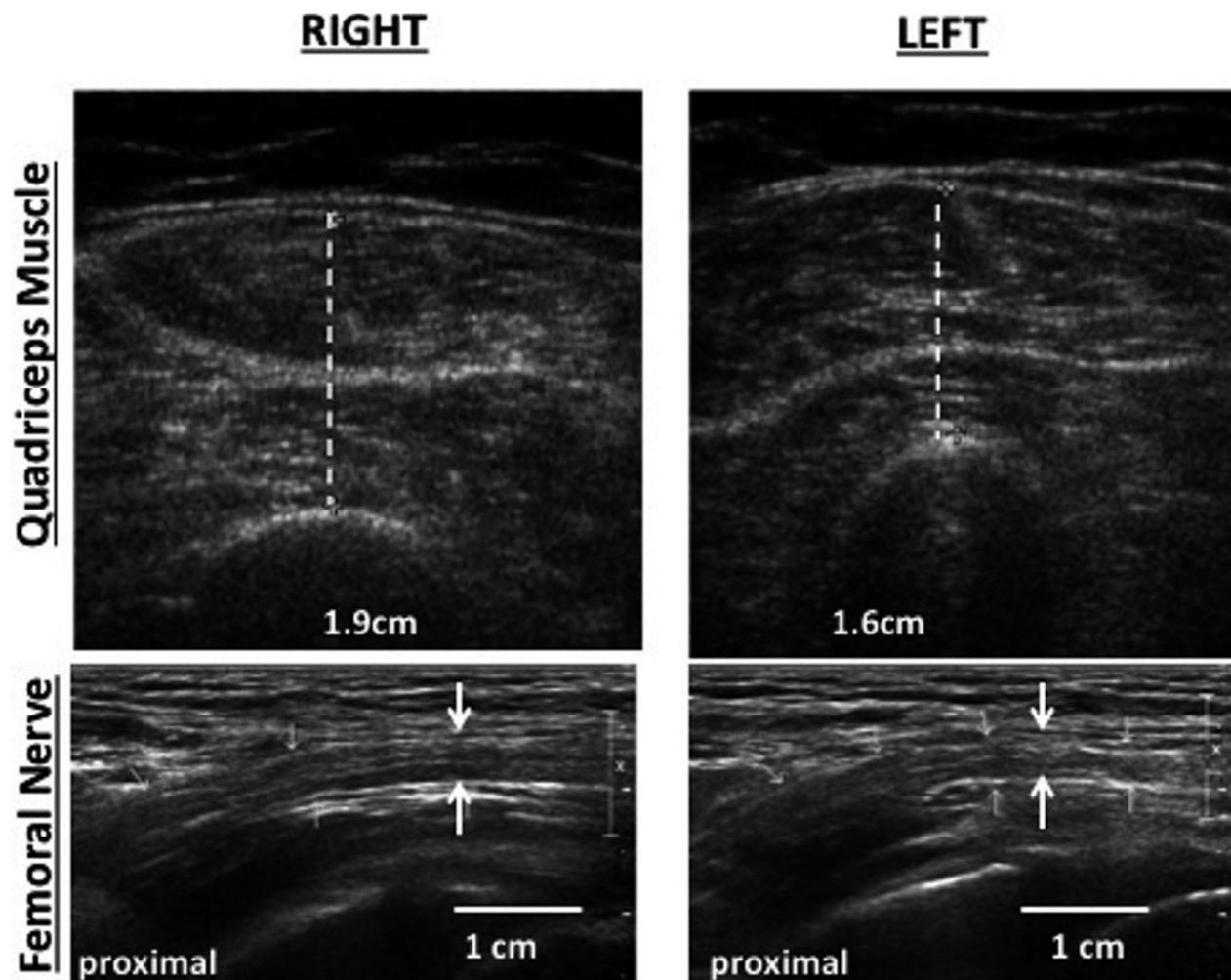

Figure 1. Ultrasound of gastrocnemius and femoral nerves. Transverse images of the quadriceps femorus muscle (top panel) obtained from younger sister show increased echointensity bilaterally and relatively reduced thickness on the left. Dotted lines demonstrate the thickness of the muscle. Longitudinal images of the femoral nerve at the inguinal ligament (bottom panel) shows bilateral nerve enlargement. Femoral nerve is shown between arrows.

infancy. Neither sister walked independently until 16–17 months of age. The older sister was diagnosed based on diffuse weakness and absent deep tendon reflexes prior to the age of 2. She was initially thought to have chronic inflammatory demyelinating polyradiculoneuropathy (CIDP), received treatment with periodic intravenous gamma globulin (IVIG) between ages 2 and 3½, but she did not improve. The IVIG was discontinued when the younger sister was also found to have neuropathy and it was realized that the neuropathy was probably genetically based. The older sister presented to us with symmetrical bilateral foot drop. She had been prescribed ankle foot orthotics (AFOs) that she initially rarely wore. At age 13, she did not consider balance to be a major problem and was falling rarely. She denied difficulties with fine hand movements such as manipulating buttons, zippers, writing, or manipulating small objects. Two years later she was falling more frequently and was using AFOs regularly, at least for longer distances. The younger sister was thought by her parents to be more severely affected in part because of asymmetrical proximal weakness of the left leg, which began to develop at between the ages of 7 and 8 years. She was diagnosed with mild hip dysplasia on the right, asymptomatic side for which she underwent surgery. However, the asymmetrical weakness on the left progressed until the left hip extensor strength was only 2/5 MRC scale. Ultrasound at age 10 showed reduced thickness of the left leg muscles including the quadriceps (Fig. 1A). However, ultrasound studies also showed enlargement of both right and left femoral nerves (Fig. 1B) as was the case with other nerves evaluated (data not shown). Additionally, ultrasound of both sisters, ages 2 and 6 years, showed diffuse nerve enlargement, with median and ulnar nerves three to five times larger than normal (data not shown). The possibility of a superimposed inflammatory component was considered at age 10 and she responded to twice weekly corticosteroid treatment with return of measurable strength in left quadriceps and iliopsoas (4/5 MRC). At age 11 years, the younger sister does use the elevator at school to go upstairs. The clinical examination of both siblings is provided in Table 1. Motor nerve conduction velocities

Table 1. Clinical features of siblings with PMP22 exon 4 deletion.

	Patient age (years)	CMTNSv2	CMT PedS	Distal weakness LL	Proximal weakness LL	Distal weakness UL	Proximal weakness UL	Vibration LL	Vibration UL	Cutaneous LL	Cutaneous UL
86687-0001	13	13 (moderate)	28	+ (4 + ,5)	− (5,5)	+(4 + .5,4 +)	− (5,5,5)	Red toes, ankles, and knees	Red fingers, wrist, and elbows	Red toes	Normal
86687-0100	9	14 (moderate)	29	+ (4-,5)	−+(2,4 +)	+ (4,5,4)	− (5,5,5)	Red toes, ankles, and knees	Red fingers, wrist, and elbows	Red toes	Normal

Motor weakness based on MRC scale (0–5): + = weakness present, − = no weakness detected. LL distal weakness assessed by anterior tibialis and gastrocnemius, LL proximal weakness assessed by Ilio psoas and quadriceps; UL distal weakness assessed by first dorsal interosseous, abductor pollicis brevis, and adductor digiti minimi, UL distal weakness assessed by deltoids, biceps brachii, and triceps. Vibration based on Rydell tuning fork with "5" on scale of "8" being considered normal and cutaneous based on pinprick sensation: Normal is no decrease compared to the examiner, Red is reduced, and abs is absent up to level indicated. Both motor and sensory evaluations were based on worst score observed of the two limbs. CMTNSv2 scores are separable into <10 (mild), 11–20 (moderate), or >20 (severe) impairment.[19] CMTPedS scores range from 0 to 44 with higher numbers suggesting greater disability.[20]

Table 2. Motor NCVs.

			Ulnar nerve				Median nerve			Peroneal nerve			
Individual	Age	Side	DML (ms) <3.4	NCV1 (m/sec) >49	NCV2 (m/sec) >50	CMAP (mV) >2.8	DML (msec) <3.5	NCV (m/sec) >48	CMAP (mV) >3.5	DML (msec) <5.5	NCV3 (m/sec) >40	NCV4 (m/sec) >40	CMAP (mV) >2.5
86687-0001	13	L	**11.3**	**7**	**10**	**1.4**	**23.4**	**9**	**0.271**	–	–	–	**NR**
86687-0100	9	L	**21.6**	**6**	**5**	**0.13**	**31.6**	**8**	**0.280**	–	–	–	–
86687-0100	9	R	**9.7**	**8**	**9**	5.3	–	–	–	–	–	–	–

Normal values for each nerve in top row under DML, NCV, and CMAP. DML, distal motor latency; NCV, nerve conduction velocity; NCV1, NCV between wrist/elbow; NCV2, NCV around elbow; NCV3, NCV between ankle/knee; NCV4, NCV around knee; CMAP, compound muscle action potential. Bold letters signify abnormal values.

(MNCV) were severely reduced to between 5 and 10 m/sec in the upper extremities for both sisters (Table 2). Sensory nerve conduction velocities were unobtainable (data not shown).

Genotyping and sequencing mutant *PMP22*

We extracted RNA from dermal nerve tissue in skin biopsies of both the older sister and an unaffected control, and then amplified the PMP22 transcript by RT-PCR. In the proband's lane, we identified two bands: a 552-bp band that migrated to the size predicted for the normal PMP22 transcript length, as seen in the positive control lane, and a 411-bp band that suggests a truncated PMP22

transcript (Fig. 2A). The 141 bp truncation was the predicted size of *PMP22* mRNA for this RT-PCR product for which exon 4 is deleted (Fig. 2B). We compared transcript sequences between the two bands; the sequencing confirmed an exon 4 in-frame deletion resulted in the smaller band, with no changes to the sequence at the PMP22 C-terminus postdeletion (Fig. 2C). Sequencing of the upper band revealed the full PMP22 coding sequence from the normal allele including exon 4. The deletion of exon 4 in the mutant transcript of our proband resulted in the loss of 47 amino acids (AA#60-106), most of which comprise the hydrophobic second transmembrane region of PMP22 protein. Translation of subsequent amino acids (AA#107-160) was not affected (Figs. 2D and 3).
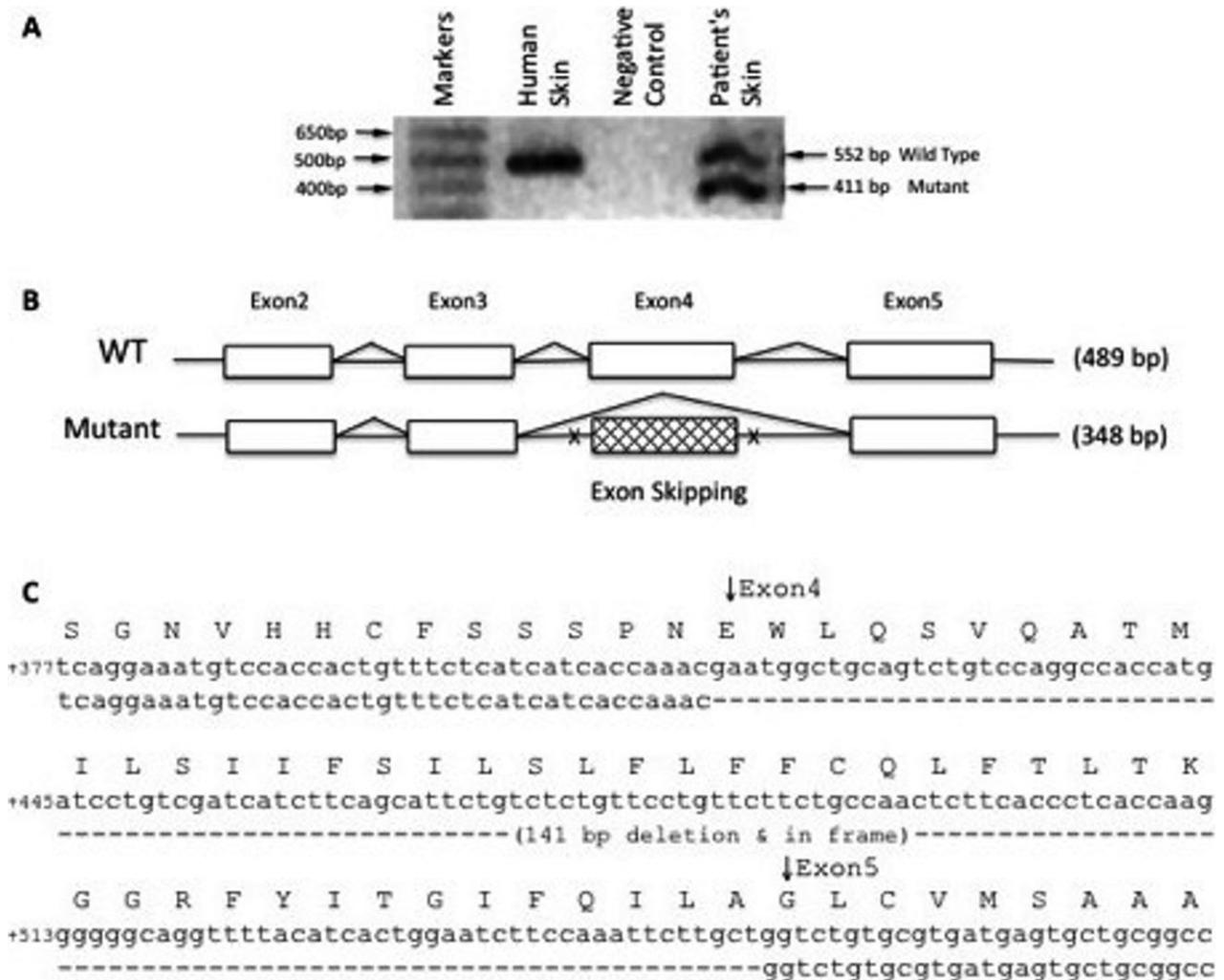

Figure 2. RT-PCR and sequencing analysis of *PMP-22* transcript. RT-PCR products amplified from RNA extracted from the proband and control skin biopsies and a control sural nerve biopsy. The band of approximately 552 bp corresponds to the normal *PMP22* transcript and the smaller band of approximately 411 bp corresponds to the misspliced *PMP22* transcript of the proband. (B) Exon–intron structure of *PMP22* shows the skipping of exon 4 caused by aa417 + 2 T>G. The nucleotide numbers in parenthesis indicate the predicted size of coding sequences for each transcript; the wild type and the mutant. (C) The PCR products were sequenced. Comparisons between wild-type and mutant transcripts demonstrate the loss of exon 4.
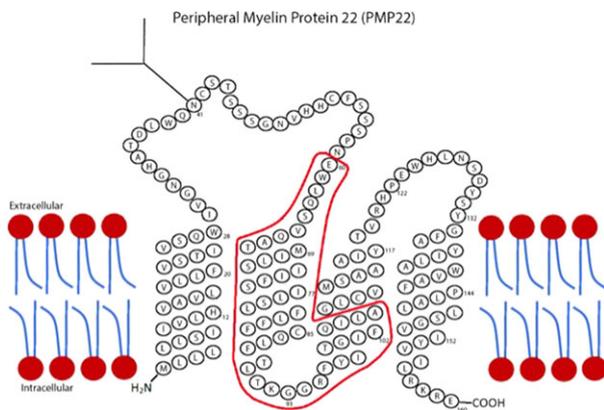
Figure 3. Peripheral myelin protein 22 (PMP22) secondary protein structure. Amino acids circled in red are encoded by exon 4 which is deleted in the patients.

PMP22Δ4 retained in ER in transfection studies

To determine the consequences of the exon 4 deletion we performed a series of transient transfection studies. We introduced the exon 4 deletion *PMP22* cDNA into two separate cultured cell lines: non-neuronal Cos7 cells and RT4 rat Schwann cells, and investigated their fate in the transfected cells. The majority of wtPMP22 in transfected Cos7 localized to the plasma membrane. PMP22Δ4 protein frequently formed aggregates intracellularly and failed to reach the plasma membrane. The aggregates colocalized with calnexin suggesting that they were retained in the endoplasmic reticulum (ER) (Fig. 4A). We observed a similar pattern in transfected RT4 Schwann cells under the same conditions (Fig. 4B).

To further quantify the above changes, we calculated the percentage of transfected cells demonstrating ER retention in both PMP22Δ4 and wild-type transfections. There was a fivefold higher percentage of Cos7 cells demonstrating retention of mutant PMP22 than retention of wtPMP22: 28% to 5.5%, respectively (Fig. 3C). There was a sixfold higher percentage of RT4 cells that revealed mutant PMP22 retention in the ER than wtPMP22 retention: 31.5% to 5%, respectively (Fig. 4C). Because the transfection efficiency was similar between PMP22Δ4 and wild-type studies, because results were similar in two separate cell types, because aggregates were much less frequent with wild-type experiments, and because studies were done in triplicate, we believe the results demonstrate that the PMP22Δ4 PMP22 mutation resulted in the intracellular aggregation we observed.

We next evaluated how the PMP22Δ4 mutation effected trafficking through the Golgi apparatus using the Golgi antibody marker (giantin). Wild-type PMP22 cDNA transfected RT4 Schwann cells displayed transport of wtPMP22 to the plasma membrane as well as some colocalization within the Golgi. PMP22Δ4, as shown above, did not travel to the plasma membrane. However, its colocalization within the Golgi did not differ from that of wild-type PMP22. Specifically, we recorded similar percentages of PMP22 colocalization with Golgi between wtPMP22 (96.2%) and PMP22Δ4 (98.7%) cDNA transfections (data not shown). Taken together, these results suggest that PMP22Δ4 is largely retained in the ER.

Discussion

We have evaluated two sisters with an unusual rearrangement within the *PMP22* gene. Although the patient's mother is mosaic for this rearrangement, and is thus clinically normal, both daughters had leg weakness beginning in infancy associated with severely slowed nerve conduction velocities of <10 m/sec, much slower than that typical for CMT1A. Consistent with the predicted data from Zhang and coworkers, based on their observations that there are exon 4 rearrangements within the PMP22 gene, our patient is missing all exon 4 sequences within the mutant PMP22 mRNA, producing a deletion of a portion of the coding region of this protein. Transfection studies with a cDNA construct encoding the mutant protein demonstrate that PMP22Δ4 is retained within the ER and is not expressed on the cell surface. Taken together, these data suggest that PMP22Δ4 causes CMT1E by a toxic gain-of-function mechanism.

Three FoSTes/MMBIR events with microhomologies at breakpoint junctions were previously identified in our patients by high-density oligonucleotide array comparative genomic hybridization (aCGH). These events were predicted to result in at least a partial deletion of exon 4.[17] Our RT-PCR, which is based on mRNA expression, confirmed this prediction by demonstrating the complete deletion of exon 4 in myelinating Schwann cells in the proband. Primers used for the RT-PCR spanned the *PMP22* gene from exon 1 to the 3′ UTR and were therefore predicted to detect any splicing abnormalities in the resultant mRNA. Since only the wild-type and exon 4 deleted bands were observed (Fig. 1), this suggested to us that the only splicing abnormality that occurred was the deletion of exon 4. Thus, in the proband, there was no evidence of variability in spliced products from the exon 4 rearrangement, and we think it unlikely that variability of splicing caused the transient asymmetry in the younger sister.

We speculated on why there were significant asymmetries in the younger sister; in particular, the quadriceps weakness of the left leg. Because the results from her sister's biopsy revealed expression of only wild-type PMP22 and PMP22Δ4, we considered it unlikely that myelinating Schwann cells ensheathing the femoral nerve from the
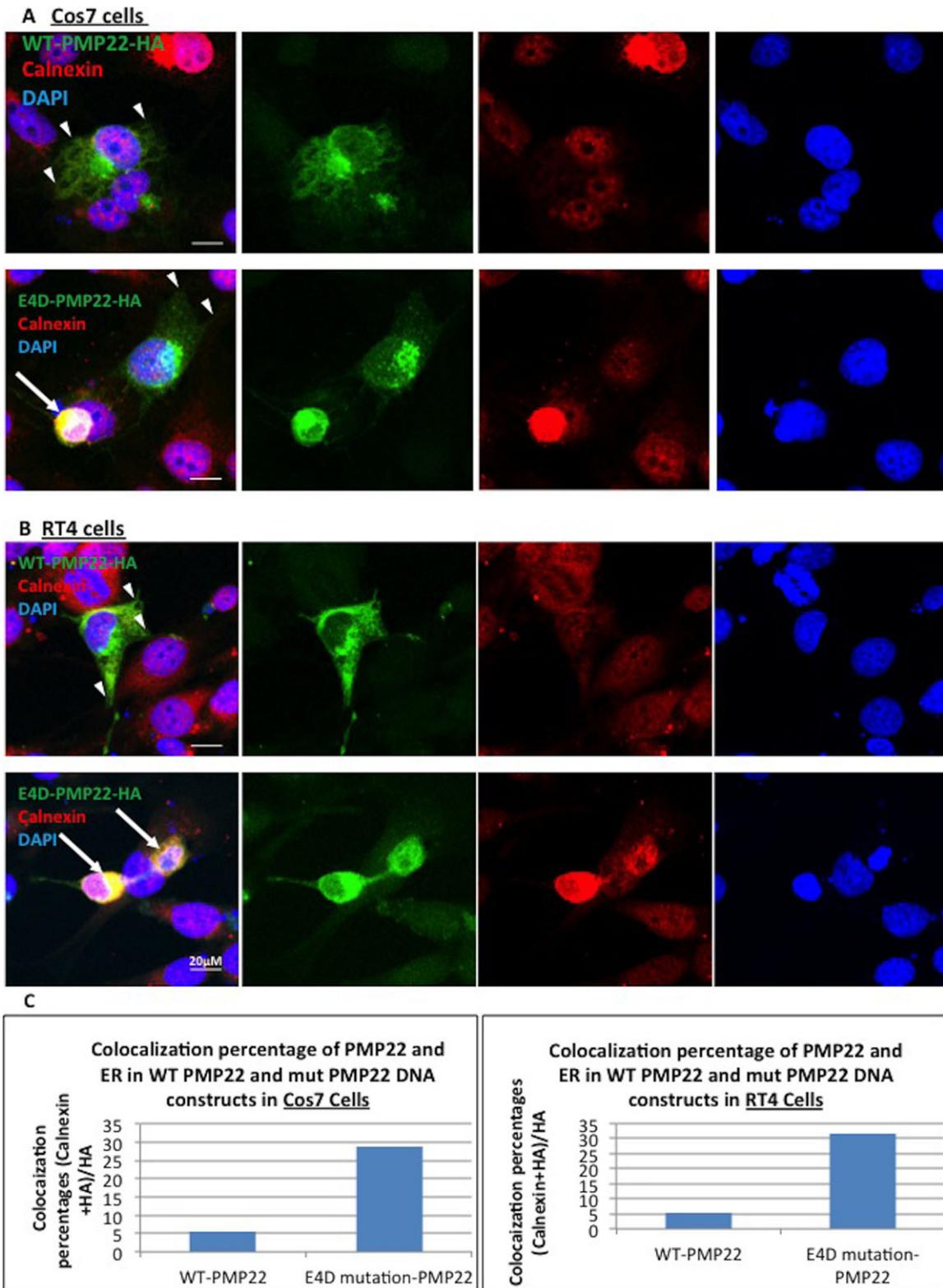
Figure 4. ER retention of PMP22Δ4. Transient transfection studies were performed in Cos7 (A) and RT4 (B) with WT PMP22 or PMP22Δ4 DNA constructs. Arrows point to PMP22Δ4 (HA) colocalization with the ER (calnexin). Arrowheads demonstrate PMP22 transported to cellular membrane. In PMP22Δ4 transfected cells, significantly more cells were retained in the ER compared to wild-type cells (C).

right leg expressed a different PMP22 mRNA than the left leg. Furthermore, ultrasound showed no asymmetry of the femoral nerves. We recognized that HNPP, which is caused by the deletion of an entire PMP22 allele, is characterized by episodes of asymmetric weakness or sensory loss, particularly at sites of compression.[18] However, there were no other features that suggested HNPP in either sibling. For example, neither sister had previously noted transient focal symptoms and their overall presentations were quite different from those of HNPP. HNPP, a clinical phenotype resulting from *PMP22* loss of function, typically has focal areas of slowing on nerve conduction studies, but outside of these regions the NCV are often nearly normal.[19] Moreover, outside of the focal episodes, most patients with HNPP have at least relatively normal neurological examinations. These two girls were not only more affected clinically than most patients with HNPP, but they were also more affected than many patients with CMT1A which is caused by *PMP22* gain of function – most often resulting from a duplication of *PMP22*. Accordingly, we hypothesized that our patients' phenotype is caused by a toxic gain of function caused by the mutant PMP22 lacking exon 4. Given the recovery of significant quadriceps function, this seems to be a superimposed problem, perhaps related to an inflammatory process. However, we were not able to explain the younger sisters asymmetries based on the specific deletion of exon 4.

Most *PMP22* missense mutations and other mutations within the *PMP22* gene cause neuropathies that are clinically more severe than CMT1A and are therefore also likely to induce toxic gain of function abnormalities in myelinating Schwann cells.[8] Mutations that cause severe neuropathies beginning in infancy are said to cause a Dejerine–Sottas syndrome (DSS) and those that prevent normal myelination are said to induce congenital hypomyelination (CHM).[8] *Met69Lys* and *Ser72Leu PMP22* have been reported to cause DSS.[20] *Ser72Leu PMP22* has also been reported to cause CHO[21] as has *Cys109Arg PMP22*[22] to provide several examples. Alternatively, other *PMP22* mutations have been reported to cause a typical HNPP phenotype. These include Leu4Ter,[9] Leu7 fs,[10,11] Gly94 fs,[12,23] Tyr97 fs,[24] and Thr99 fs[25] *PMP22*. Mutations that cause an HNPP phenotype eliminate the mutant allele by processes such as nonsense-mediated decay.[11,26] Thus, these are complete loss-of-function alleles similar to traditional HNPP in which the PMP22 allele is deleted.[13] How other mutations cause a gain of function is not known, but clues about mechanisms can be inferred from studies performed in the naturally occurring Trembler (Tr) and Trembler J (Tr[J]) mouse models of CMT1E. Tr and Tr[J] result from Gly150Asp[27] and Leu16Pro PMP22,[28] respectively. Both Tr[29] and Tr[J30,31]

mutations cause DSS in humans, and the mice can be used to model the human neuropathies. Leu16Pro PMP22 has been shown to be retained in the ER of Schwann cells in Tr[J] mice.[32] Moreover, the mice have demonstrated improvement following treatment with curcumin to reduce ER stress.[32] Similar results have been found in two missense mutations in myelin protein zero (MPZ) that cause CMT1B. The Ser63del and Arg98Cys MPZ mutations causing CMT1B are retained within the ER and are thought to cause neuropathy in part by activating the unfolded protein response (UPR) secondary to ER stress.[33,34] The three arms of the UPR work together in part to relieve ER stress by reducing the overall translation of proteins by the cell.[35] Therapies directed at relieving ER stress and attenuating the UPR have improved the neuropathy of both Ser63del[33,36] and Arg98Cys[16] mice. Our data suggest that this process may also occur with *PMP22Δ4*, further expanding the role of ER stress and UPR activation in the pathogenesis of what are often more severe forms of CMT1.

Acknowledgments

Authors' Contributions

Mr. Wang, Dr. Wu, and Dr. Bai performed the experiments involved in cloning, tissue culture, transfections, and RT-PCR studies. Dr. Zaidman performed the ultrasound studies and was involved in the interpretation of the data. Dr. Kamholz and Lupski were involved in the interpretation of the data and in the writing of the manuscript. Dr. Connolly was involved in evaluating the patients and analyzing their clinical phenotype. Ms. Grider was involved in caring for and evaluating the family as well as contributing to the writing of the paper. Dr. Shy designed the experiments, evaluated the patients and designed, and was the primary writer of the manuscript.

Conflicts of Interest

Dr. Lupski: Baylor College of Medicine (BCM) and Miraca Holdings, Inc., have formed a joint venture with

shared ownership and governance of Baylor Genetics (BG), formerly the Baylor Miraca Genetics Laboratories (BMGL), which performs clinical exome sequencing. J. R. L. is an employee of BCM, serves on the Scientific Advisory Board of the BG, and derives support through a professional services agreement with the BG. JRL has stock ownership in 23andMe, is a paid consultant for Regeneron Pharmaceuticals, has stock options in Lasergen, Inc., and is a coinventor on multiple United States and European patents related to molecular diagnostics for inherited neuropathies, eye diseases, and bacterial genomic fingerprinting.

References

1. Skre H. Genetic and clinical aspects of Charcot-Marie-tooth's disease. Clin Genet 1974;6:98–118.

2. Fridman V, Bundy B, Reilly MM, et al. CMT subtypes and disease burden in patients enrolled in the Inherited Neuropathies Consortium natural history study: a cross-sectional analysis. J Neurol Neurosurg Psychiatry 2015;86:873–878.

3. Lupski JR, de Oca-Luna RM, Slaugenhaupt S, et al. DNA duplication associated with Charcot-marie-tooth disease type 1A. Cell 1991;66:219–232.

4. Timmerman V, Nelis E, Van Hul W, et al. The peripheral myelin protein gene PMP-22 is contained within the Charcot-Marie-Tooth disease type 1A duplication. Nat Genet 1992;1:171–175.

5. Lupski JR, Stankiewicz P. Genomic disorders: molecular mechanisms for rearrangements and conveyed phenotypes. PLoS Genet 2005;1:e49.

6. Pentao L, Wise CA, Chinault AC, et al. Charcot-Marie-Tooth type 1A duplication appears to arise from recombination at repeat sequences flanking the 1.5 Mb monomer unit. Nat Genet 1992;2:292–300.

7. Lupski JR. Structural variation mutagenesis of the human genome: Impact on disease and evolution. Environ Mol Mutagen 2015;56:419–436.

8. Shy M, Lupski JR, Chance PF, et al. The Hereditary motor and sensory neuropathies: an overview of the clinical, genetic, electrophysiologic and pathlogic features. In: Dyck PJTP, ed. Peripheral Neuropathy, 4th ed. Philadelphia: WB Saunders, 2005:1623–1658.

9. Muglia M, Patitucci A, Rizzi R, et al. A novel point mutation in PMP22 gene in an Italian family with hereditary neuropathy with liability to pressure palsies. J Neurol Sci 2007;263:194–197.

10. Nicholson GA, Valentijn LJ, Cherryson AK, et al. A frame shift mutation in the PMP22 gene in hereditary neuropathy with liability to pressure palsies. Nat Genet 1994;6:263–266.

11. Li J, Ghandour K, Radovanovic D, et al. Stoichiometric alteration of PMP22 protein determines the phenotype of hereditary neuropathy with liability to pressure palsies. Arch Neurol 2007;64:974–978.

12. Lenssen PP, Gabreels-Festen AA, Valentijn LJ, et al. Hereditary neuropathy with liability to pressure palsies. Phenotypic differences between patients with the common deletion and a PMP22 frame shift mutation. Brain 1998;121(Pt 8):1451–1458.

13. Chance PF, Alderson MK, Leppig KA, et al. DNA deletion associated with hereditary neuropathy with liability to pressure palsies. Cell 1993;72:143–151.

14. Zhang F, Seeman P, Liu P, et al. Mechanisms for nonrecurrent genomic rearrangements associated with CMT1A or HNPP: rare CNVs as a cause for missing heritability. Am J Hum Genet 2010;86:892–903.

15. Sabet A, Li J, Ghandour K, et al. Skin biopsies demonstrate MPZ splicing abnormalities in Charcot-Marie-Tooth neuropathy 1B. Neurology 2006;67:1141–1146.

16. Patzko A, Bai Y, Saporta MA, et al. Curcumin derivatives promote Schwann cell differentiation and improve neuropathy in R98C CMT1B mice. Brain 2012;135:3551–3566.

17. Zhang F, Khajavi M, Connolly AM, et al. The DNA replication FoSTeS/MMBIR mechanism can generate genomic, genic and exonic complex rearrangements in humans. Nat Genet 2009;41:849–853.

18. Li J, Krajewski K, Lewis RA, Shy ME. Loss-of-function phenotype of hereditary neuropathy with liability to pressure palsies. Muscle Nerve 2004;29:205–210.

19. Li J, Krajewski K, Shy ME, Lewis RA. Hereditary neuropathy with liability to pressure palsy: the electrophysiology fits the name. Neurology 2002;58:1769–1773.

20. Roa BB, Dyck PJ, Marks HG, et al. Dejerine-Sottas syndrome associated with point mutation in the peripheral myelin protein 22 (PMP22) gene. Nat Genet 1993;5:269–273.

21. Simonati A, Fabrizi GM, Pasquinelli A, et al. Congenital hypomyelination neuropathy with Ser72Leu substitution in PMP22. Neuromuscul Disord 1999;9:257–261.

22. Fabrizi GM, Simonati A, Taioli F, et al. PMP22 related congenital hypomyelination neuropathy. J Neurol Neurosurg Psychiatry 2001;70:123–126.

23. Young P, Wiebusch H, Stogbauer F, et al. A novel frameshift mutation in PMP22 accounts for hereditary neuropathy with liability to pressure palsies. Neurology 1997;48:450–452.

24. Yurrebaso I, Casado OL, Barcena J, et al. Clinical, electrophysiological and magnetic resonance findings in a family with hereditary neuropathy with liability to pressure palsies caused by a novel PMP22 mutation. Neuromuscul Disord 2014;24:56–62.

25. Moszynska I, Kabzinska D, Sinkiewicz-Darol E, Kochanski A. A newly identified Thr99fsX110 mutation in the PMP22 gene associated with an atypical phenotype of the

hereditary neuropathy with liability to pressure palsies. Acta Biochim Pol 2009;56:627–630.

26. Khajavi M, Inoue K, Lupski JR. Nonsense-mediated mRNA decay modulates clinical outcome of genetic disease. Eur J Hum Genet 2006;14:1074–1081.

27. Suter U, Welcher AA, Ozcelik T, et al. Trembler mouse carries a point mutation in a myelin gene. Nature 1992;356:241–244.

28. Suter U, Moskow JJ, Welcher AA, et al. A leucine-to-proline mutation in the putative first transmembrane domain of the 22-kDa peripheral myelin protein in the trembler-J mouse. Proc Natl Acad Sci USA 1992;89:4382–4386.

29. Ionasescu VV, Searby CC, Ionasescu R, et al. Dejerine-Sottas neuropathy in mother and son with same point mutation of PMP22 gene. Muscle Nerve 1997;20:97–99.

30. Valentijn LJ, Baas F, Wolterman RA, et al. Identical point mutations of PMP-22 in Trembler-J mouse and Charcot-Marie-Tooth disease type 1A. Nat Genet 1992;2:288–291.

31. Hoogendijk JE, Janssen EA, Gabreels-Festen AA, et al. Allelic heterogeneity in hereditary motor and sensory neuropathy type Ia (Charcot-Marie-Tooth disease type 1a). Neurology 1993;43:1010–1015.

32. Khajavi M, Shiga K, Wiszniewski W, et al. Oral curcumin mitigates the clinical and neuropathologic phenotype of the Trembler-J mouse: a potential therapy for inherited neuropathy. Am J Hum Genet 2007;81:438–453.

33. Pennuto M, Tinelli E, Malaguti M, et al. Ablation of the UPR-Mediator CHOP restores motor function and reduces demyelination in Charcot-Marie-Tooth 1B mice. Neuron 2008;57:393–405.

34. Saporta MA, Shy BR, Patzko A, et al. MpzR98C arrests Schwann cell development in a mouse model of early-onset Charcot-Marie-Tooth disease type 1B. Brain 2012;135:2032–2047.

35. Rutkowski DT, Kaufman RJ. A trip to the ER: coping with stress. Trends Cell Biol 2004;14:20–28.

36. Das I, Krzyzosiak A, Schneider K, et al. Preventing proteostasis diseases by selective inhibition of a phosphatase regulatory subunit. Science 2015;348:239–242.